Early and middle Miocene Antarctic glacial history from the sedimentary facies distribution in the AND-2A drill hole, Ross Sea, Antarctica

Article *in* Geological Society of America Bulletin · April 2011

CITATIONS
26

READS
74

62 authors, including:

Sandra Passchier
Montclair State University
154 PUBLICATIONS **3,003** CITATIONS
SEE PROFILE

B. Field
Retired
77 PUBLICATIONS **1,553** CITATIONS
SEE PROFILE

Christopher R. Fielding
University of Nebraska at Lincoln
351 PUBLICATIONS **10,779** CITATIONS
SEE PROFILE

Kurt S. Panter
Bowling Green State University
75 PUBLICATIONS **1,356** CITATIONS
SEE PROFILE

Geological Society of America Bulletin

Early and middle Miocene Antarctic glacial history from the sedimentary facies distribution in the AND-2A drill hole, Ross Sea, Antarctica

S. Passchier, G. Browne, B. Field, C.R. Fielding, L.A. Krissek, K. Panter, S.F. Pekar and and ANDRILL-SMS Science Team

Geological Society of America Bulletin 2011;123, no. 11-12;2352-2365
doi: 10.1130/B30334.1

Notes

Early and middle Miocene Antarctic glacial history from the sedimentary facies distribution in the AND-2A drill hole, Ross Sea, Antarctica

S. Passchier[1,*], G. Browne[2], B. Field[2], C.R. Fielding[3], L.A. Krissek[4], K. Panter[5], S.F. Pekar[6], and ANDRILL-SMS Science Team[†]

[1]*Department of Earth and Environmental Studies, Montclair State University, Montclair, New Jersey 07043, USA*
[2]*GNS Science, PO Box 30-368, Lower Hutt 5040, New Zealand*
[3]*Department of Earth and Atmospheric Sciences, University of Nebraska, Lincoln, Nebraska 68588, USA*
[4]*School of Earth Sciences, The Ohio State University, Columbus, Ohio 43210, USA*
[5]*Department of Geology, Bowling Green State University, Bowling Green, Ohio 43403, USA*
[6]*School of Earth and Environmental Sciences, Queens College, City University of New York, Flushing, New York 11367, USA*

ABSTRACT

In 2007, the Antarctic Geological Drilling Program (ANDRILL) drilled 1138.54 m of strata ~10 km off the East Antarctic coast, including an expanded early to middle Miocene succession not previously recovered from the Antarctic continental shelf. Here, we present a facies model, distribution, and paleoclimatic interpretation for the AND-2A drill hole, which enable us, for the first time, to reconstruct periods of early and middle Miocene glacial advance and retreat and paleoenvironmental changes at an ice-proximal site. Three types of facies associations can be recognized that imply significantly different paleoclimatic interpretations. (1) A diamictite-dominated facies association represents glacially dominated depositional environments, including subglacial environments, with only brief intervals where ice-free coasts existed, and periods when the ice sheet was periodically larger than the modern ice sheet. (2) A stratified diamictite and mudstone facies association includes facies characteristic of open-marine to iceberg-influenced depositional environments and is more consistent with a very dynamic ice sheet, with a grounding line south of the modern position. (3) A mudstone-dominated facies association generally lacks diamictites and was produced in a glacially influenced hemipelagic depositional environment. Based on the distribution of these facies associations, we can conclude that the Antarctic ice sheets were dynamic, with grounding lines south of the modern location at ca. 20.1–19.6 Ma and ca. 19.3–18.7 Ma and during the Miocene climatic optimum, ca. 17.6–15.4 Ma, with ice-sheet and sea-ice minima at ca. 16.5–16.3 Ma and ca. 15.7–15.6 Ma. While glacial minima at ca. 20.1–19.6 Ma and ca. 19.3–18.7 Ma were characterized by temperate margins, an increased abundance of gravelly facies and diatomaceous siltstone and a lack of meltwater plume deposits suggest a cooler and drier climate with polythermal conditions for the Miocene climatic optimum (ca. 17.6–15.4 Ma). Several periods of major ice growth with a grounding line traversing the drill site are recognized between ca. 20.2 and 17.6 Ma, and after ca. 15.4 Ma, with evidence of cold polar glaciers with ice shelves. The AND-2A core provides proximal evidence that during the middle Miocene climate transition, an ice sheet larger than the modern ice sheet was already present by ca. 14.7 Ma, ~1 m.y. earlier than generally inferred from deep-sea oxygen isotope records. These findings highlight the importance of high-latitude ice-proximal records for the interpretation of far-field proxies across major climate transitions.

INTRODUCTION

Background

The Antarctic ice sheets are an important component of the global climate system because of their influence on sea-ice formation, ocean circulation, and latitudinal temperature gradients. Additionally, changes in the volume of continental ice have controlled global sea level throughout the past ~35 m.y. (Zachos et al., 2001; Naish et al., 2001, Miller et al., 2005). The middle Miocene climate transition signaled a major shift in Earth's climate evolution, characterized by one of the three large Cenozoic stepwise increases in $\delta^{18}O$, resulting from a combination of global cooling and ice growth in Antarctica (Zachos et al., 2001). Multiple Miocene oxygen isotope events, labeled Mi1–Mi7, have been recognized by others and have been attributed to Antarctic glacial events (Miller et al., 1991) with ice volumes periodically larger than today (Pekar and DeConto, 2006). Modeling studies demonstrate that Antarctic ice growth is governed by atmospheric pCO_2 thresholds (DeConto and Pollard, 2003), and although pCO_2 values appear to have dropped off after ca. 25 Ma (Pagani et al., 2005), pCO_2 reached a maximum, with possibly higher than present-day levels, in the middle Miocene (Tripati et al., 2009). Documenting changes in Antarctic ice volume through these climate transitions is essential in understanding future responses to the rising pCO_2.

Magnesium/calcium (Mg/Ca) and high-resolution stable isotope records suggest that Antarctica experienced relatively reduced ice conditions during the Miocene climatic optimum ca. 17–15 Ma and that sea-surface temperatures in the Southern Ocean were variable (Lear et al., 2000; Billups and Schrag, 2002; Shevenell et al., 2004; Holbourn et al., 2005). In the Southern Ocean, a 6–7 °C cooling is observed in the record between 14.2 and 13.8 Ma, followed by a major increase in Antarctic ice volume at 13.8 Ma (Shevenell et al., 2004; Holbourn et al., 2005). Mg/Ca records, however, are affected by uncertainties concerning variation in Mg/Ca ratios of the ocean surface through time (Billups and Schrag, 2002; Lear et al., 2004, 2008). Therefore, providing ground-truth for these records through the investigation of ice-proximal strata on the Antarctic continental margin is a necessity.

*E-mail: passchiers@mail.montclair.edu
[†]See http://www.andrill.org/projects/sms/team.html

GSA Bulletin; November/December 2011; v. 123; no. 11/12; p. 2352–2365; doi: 10.1130/B30334.1; 10 figures; 1 table.

Drill holes on the Antarctic margin document a significant, but gradual, change in Antarctic paleoclimate and ice-sheet dynamics across the Oligocene-Miocene boundary, characterized by a cooling trend, a decline in continental weathering and cool-temperate vegetation, and the establishment of an orbitally influenced dynamic continental ice sheet of modern proportions (Naish et al., 2001; Ehrmann et al., 2005; Barrett, 2007; Passchier and Krissek, 2008; Wilson et al., 2009). Until recently, the early and middle Miocene glacial record of the Antarctic margin was incomplete due to the presence of hiatuses in drill holes, presumably caused by glacial erosion on the Antarctic continental shelf. The timing of formation of a dry-based, quasi-permanent ice sheet in East Antarctica during this time has been a subject of great controversy. Some have proposed that the East Antarctic Ice Sheet became a stable, dry-based ice sheet in the middle Miocene (ca. 14 Ma) (Marchant et al., 1993; Sugden and Denton, 2004), whereas others prefer a scenario wherein periods of warming resulted in periodic changes to more dynamic wet-based glacial conditions, with a transition to a more permanent dry-based polar ice sheet as late as ca. 3 Ma (Harwood, 1986; Harwood and Webb, 1998; Hambrey and McKelvey, 2000; Joseph et al., 2002; Whitehead et al., 2006; Rebesco et al., 2006). Based on geomorphological studies in the Dry Valleys, Lewis et al. (2007) suggested that wet-based glacial conditions dominated in East Antarctica during the Miocene climatic optimum (15–17 Ma), followed by a transition to dry-based glacial conditions prior to 13.94 Ma.

To obtain a more complete proximal stratigraphic record of Miocene ice-sheet development, the Antarctic Geological Drilling Program (ANDRILL), drilled a 1138.54-m-deep hole (AND-2A) in southern McMurdo Sound in 2007 (Fig. 1). The recovered strata range in age from early Miocene to Pleistocene and include an expanded lower and middle Miocene section, not previously recovered from the Antarctic continental shelf. With the present record from AND-2A, we are able to provide a detailed reconstruction of Antarctic ice-sheet dynamics for the early and middle Miocene epoch. Here, we present a facies model and an analysis of the facies distribution of AND-2A and discuss their implications for the interpretation of far-field records of eustatic sea-level and ice-volume proxies.

Location and Geological Setting

Within southern McMurdo Sound, Ross Sea embayment, AND-2A (77°45.488′S, 165°16.605′E) recovered 98% of an 1138.54-m-thick sedimentary succession within a current water depth of ~380 m. The AND-2A core was drilled from a fast-ice platform adjacent to the Transantarctic Mountains into the margin of the Victoria Land Basin, both of which are part of the West Antarctic Rift system. Accommodation for sediment was created through fault- and flexure-related subsidence associated with rifting. Regional seismic-reflection surveys show that the penetrated succession is composed of a series of clinoform sets produced by uplift and erosion as a result of renewed rifting of the Terror Rift (Fielding et al., 2008a). Sediment was supplied by alpine glaciers or outlet glaciers draining the East Antarctic Ice Sheet by traversing the Transantarctic Mountains to the west, or from the West Antarctic Ice Sheet and Ross Ice Shelf to the south. The active rifting and passive thermal subsidence during the early and middle Miocene produced the accommodation space for the accumulation of this Neogene succession (Fielding et al., 2008a).

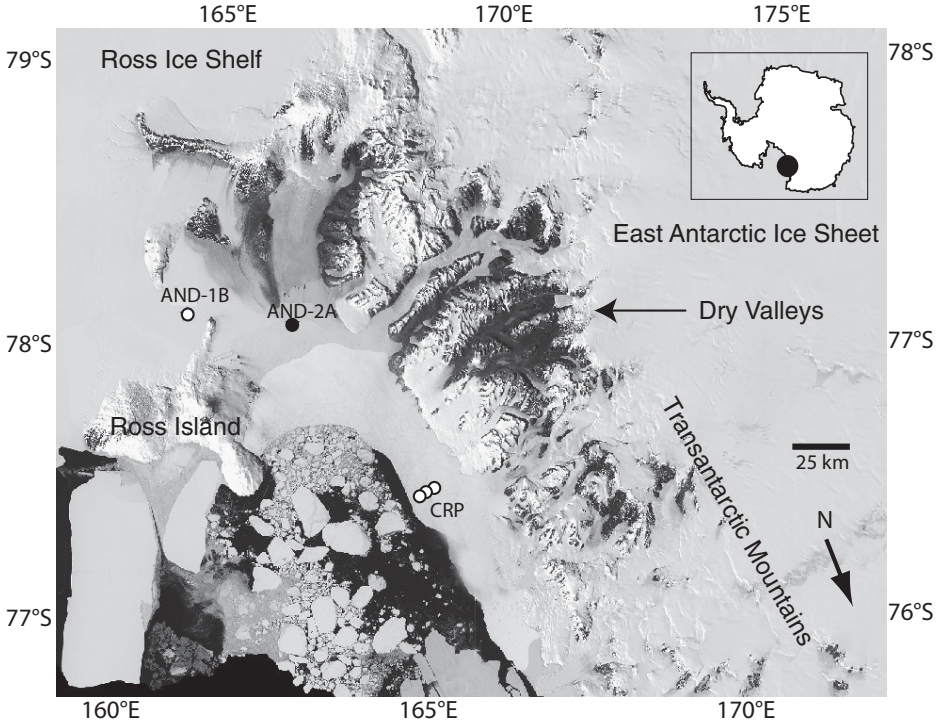

Figure 1. Location of AND-2A drill site in Southern McMurdo Sound. The AND-1B and Cape Roberts Drilling Project (CRP) drill sites are also indicated.

Sedimentary Processes

Today, southern McMurdo Sound is the terminal area of the Ross Ice Shelf, which originates from outlet glaciers of the East Antarctic Ice Sheet and ice streams draining the West Antarctic Ice Sheet. The East Antarctic Ice Sheet is regarded as a dry-based polar ice sheet largely frozen to its bed at its margin. Facies described from cores collected beneath and in front of East Antarctic ice shelves are composed of clast-rich muddy diamictons with low concentrations of diatom fragments (Domack and Harris, 1998; Evans and Pudsey, 2002; Domack et al., 2005; Hemer et al., 2007; McKay et al., 2008). These are deposited either subglacially or by melt-out from the basal debris zone proximal to the grounding line but away from the direct influence of currents (Domack and Harris, 1998; McKay et al., 2008). Under an ice shelf, interlaminated sands and silts with cross-bedding occur when sub–ice-shelf currents are generated by tidal pumping and thermohaline flow in a narrow cavity near the grounding line (Domack and Harris, 1998; Hemer et al., 2007).

Recent studies show that the West Antarctic Ice Sheet periodically collapsed during the Neogene, markedly changing ice-flow patterns in the region and periodically creating conditions of open-marine sedimentation in southern McMurdo Sound (Naish et al., 2009). During these times, fjordal conditions with advancing and retreating tidewater glaciers existed in the transverse valleys of the Transantarctic Mountains, including the Dry Valleys (McKelvey, 1981, 1982; Powell, 1981; Webb and Wrenn, 1982; Ishman and Rieck, 1992; Barrett and Hambrey, 1992; Prentice et al., 1993). Where

fast-flowing outlet glaciers from a major ice sheet terminate in a continental shelf environment, such as on the Polar North Atlantic and Alaska margins, thick stratified diamictons are deposited over large portions of the continental shelf (Powell and Molnia, 1989; Dowdeswell et al., 1998; Ó Cofaigh et al., 2001). Grounded temperate tidewater termini produce morainal bank systems composed of diamictons and gravel, and gravity flow–influenced sands and muds (Powell and Molnia, 1989; Cai et al., 1997). Upon glacial retreat, laminated and bioturbated muds and fine sands are deposited from surface plumes with a fluvial or glaciofluvial source (Powell and Molnia, 1989; Svendsen et al., 1992; Cowan et al., 1997; Dowdeswell et al., 1998; Ó Cofaigh and Dowdeswell, 2001; Powell and Cooper, 2002; Lowe and Anderson, 2002). In wave-dominated, shallow-marine settings, formerly glaciofluvial sands may be reworked into storm beds with hummocky and swaley cross-stratification (Powell and Molnia, 1989). Carbonate macrofossils can be quite abundant, and biogenic productivity is generally high, but the concentrations of siliceous microfossils in the sediments can be low in temperate glacial settings due to the high terrigenous sedimentation rates (Powell and Molnia, 1989; Dowdeswell et al., 1998).

Both temperate and polythermal glaciers produce significant amounts of meltwater, but polythermal glaciers generally have cold margins, reducing the efficiency of glacial comminution (Hambrey et al., 1999). Although distinguishing between modern glaciomarine facies produced by Arctic temperate (Alaskan) and polythermal (East Greenland, Svalbard) outlet glaciers has proved to be difficult, a dominance of gravel-rich facies in ice-distal records suggests a larger role for iceberg sedimentation consistent with colder conditions (Svendsen et al., 1992; Dowdeswell et al., 1998; Smith and Andrews, 2000; Ó Cofaigh et al., 2001). Studies of modern terrestrial environments demonstrate the volumetric importance of sandy gravel lithofacies originating as glaciofluvial bed load in ice-proximal deposits of polythermal glaciers (Etienne et al., 2003). Further, modern subpolar Antarctic bays and fjords seem to be affected by a reduced terrigenous supply, as indicated by an increase in diatomaceous muds and oozes in the distal glaciomarine environment coincident with decreasing temperature and precipitation (Griffith and Anderson, 1989). Facies associations deposited over glacial-interglacial cycles near polythermal glaciers, therefore, are expected to contain larger volumes of sandy gravel and diamictites, smaller volumes of laminated meltwater deposits, and a larger proportion of biogenic silica in ice-distal muds, compared to those originating in temperate glacial settings.

Based on a comparison with modern analogs, we analyzed the distribution of facies in the AND-2A core and identified broad periods of ice advance and retreat and changes in paleoenvironmental conditions from this .ice-proximal record. Although we recognize that both changes in bathymetry and ice extent influence sedimentary facies associations and stratigraphic stacking patterns, we focus here on the imprint of glacial variations on the environments of deposition.

METHODS

Graphic logs of the section were compiled from the cut face of the core, recording lithology, bed contacts, physical and biogenic sedimentary structures, presence of fossils, and any other features of note (Fielding et al., 2008b). Terminology refers to lithified forms (suffix "-stone" or "-ite," although the upper ~840 m of the cored section is largely unlithified, but strongly compacted). The uppermost 229.24 m below seafloor (mbsf) were drilled with a PQ drill string, generating core with an average diameter of 8.3 cm. From 229.24 to 1011.04 mbsf, an HQ drill string was used (core diameter 6.1 cm). Below 1011.04 mbsf, an NQ drill string recovered core with an average diameter of 4.5 cm. In our classification scheme, diamictites are poorly sorted sedimentary rocks with >1% gravel-sized clasts (after Moncrieff, 1989). The term "diamictite" hence is used here as a textural term, without any genetic connotations. Clast percentages were estimated visually using a comparison chart. Numbers of clasts (>2 mm) were also counted per core section (1 m long) and were normalized to account for differences in recovered section length and core width (PG, HQ, or NQ drill string). Smear slides at ~1 m intervals were used to estimate biogenic and volcanic components in the matrix of fine-grained sediments (Panter et al., 2008). The preliminary chronology of the core is based on a combination of Ar-Ar geochronology of volcanic material, diatom, and foraminifer biostratigraphy, magnetostratigraphy, and Sr isotope chronology of pristine shell material (Acton et al., 2008; Di Vincenzo et al., 2010; Fig. 2).

FACIES ANALYSIS

Nine nonvolcanic sedimentary facies were identified on the basis of lithology, sedimentary structures, bed contacts, stratigraphic relationships, and fossil content (Table 1); four facies consisting of primary volcanic rocks and volcaniclastic sedimentary rocks present in the upper 37 m of the AND-2A site are discussed in detail elsewhere (Del Carlo et al., 2009; Di Vincenzo et al., 2010). Some facies are moderately bioturbated, and ichnofossils mainly consist of *Asterosoma*, *Chondrites*, *Planolites*, *Palaeophycus*, *Teichichnus*, and rarely *Ophiomorpha*, indicative of neritic environments. Calcareous macrofossils consist of serpulid polychaete worm tubes, bivalve and gastropod shell fragments, bryozoa, and foraminifera.

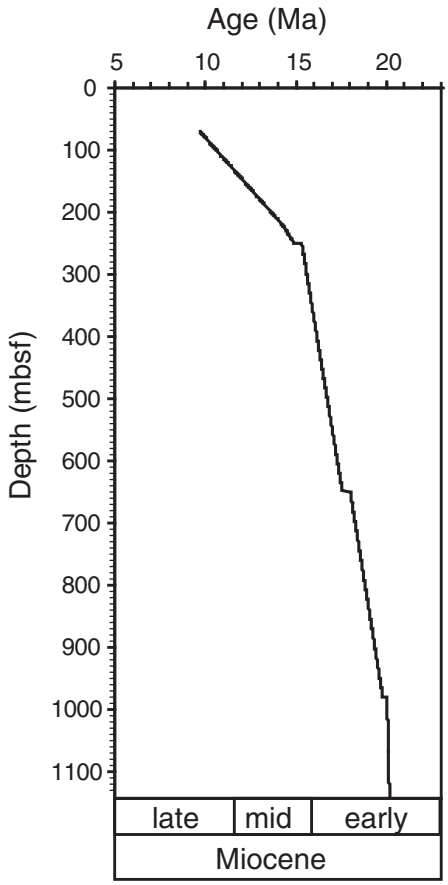

Figure 2. Age model for AND-2A, based on magnetostratigraphy (mbsf—m below seafloor) constrained by Ar-Ar geochronology of volcanic material, diatom, and foraminifer biostratigraphy, and Sr-isotope chronology of pristine shell material (Acton et al., 2008; Di Vincenzo et al., 2010).

Fine-Grained Facies Indicating Hemipelagic Sedimentation

Three facies are massive with minor laminated intervals and variable clast percentages and with clasts generally appearing as clast clusters. The facies differ in biogenic silica and macrofossil content, sand and gravel content, and intensity of bioturbation (Table 1).

(1) The diatomaceous siltstone (Z) lithofacies consists of diatomite, clast-bearing

TABLE 1. FACIES DESCRIPTION AND INTERPRETATION

Facies	Lithology	Structure	Clast (%)	Silica* (%)	Fossils†	Paleoenvironment
Z	Diatomaceous siltstone	Massive	<1–5	10–95	Rare	Pelagic and hemipelagic with ice rafting
Zb	Siltstone	Bioturbated	Rare	<18	Common	Hemipelagic with rare ice rafting
MSm	Muddy sandstone	Massive/laminated	<1	<10	Rare	Hemipelagic with significant ice rafting
Ss	Sandstone	Stratified	Rare	Trace	Rare	Wave- or current-influenced environment
SMs	Sandstone/mudstone	Interstratified	Rare	Trace	Rare	Ice-influenced delta top/front
SZs	Sandstone/siltstone	Interlaminated	<1	Trace	Absent	Ice-proximal meltwater plumes
Ds	Diamictite	Stratified	1–40	Trace	Present	Ice-proximal to ice-distal glaciomarine
Dm	Diamictite	Massive	1–40	Trace	Rare	Ice-proximal glaciomarine or subglacial
G	Conglomerate/sandstone	Stratified/massive	>40	Trace	Present	Ice-proximal glaciofluvial, ice-shelf collapse

*Refers to biogenic silica content.
†Refers to calcareous macrofossils.

siltstone, and diamictite with a matrix composed of siliceous microdebris of whole or fragmented diatoms and sponge spicules. This facies is massive or laminated at a millimeter-scale, locally moderately bioturbated, and has loaded upper contacts and sharp and inclined lower contacts (Fig. 3).

(2) The bioturbated siltstone (Zb) lithofacies is composed of moderately to extensively bioturbated clayey siltstone, sandy siltstone, or silty very fine sandstone, with up to 18% biogenic silica and common calcareous macrofossils (Fig. 3). Bed contacts are generally sharp and loaded or irregular at the top and sharp but planar at the bottom. Thinner massive beds coarsen upward from clayey siltstone to sandy siltstone and are bioturbated at the top. Thicker beds generally include <1-m-scale subtle alternations in particle size and interbedded (1) bioturbated intervals, (2) intervals that appear massive or structureless, and (3) intervals with reminiscent millimeter-scale lamination and rare soft-sediment deformation or microfaulting. Outsized clasts are absent or rare and, if present, are up to granule size.

(3) The muddy sandstone with clasts (MSm) lithofacies consists of moderately to poorly sorted, fine to very fine muddy sandstone or sandy mudstone with dispersed clasts (Fig. 3). This facies is predominantly massive, but locally weakly stratified with gravel, sand, or mud laminae on a millimeter to centimeter scale. Thin decimeter-scale interbeds of diamictite are common, and thin decimeter-scale graded sand beds occur locally. Stratified intervals are locally soft-sediment folded or microfaulted, and laminae are often disrupted or discontinuous. Clast percentages are <1%, and clast sizes are typically up to pebble grade, with a dominance of granule-sized clasts. Some beds have a dominant proportion of volcanic clasts, primarily scoria and pumice granules.

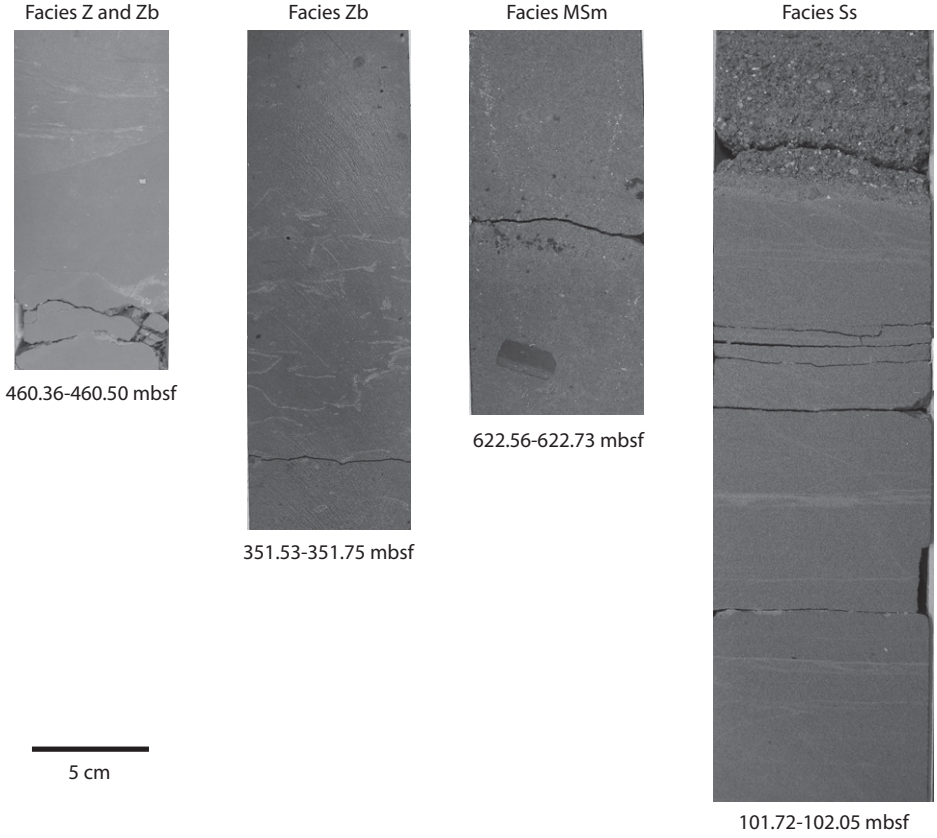

Figure 3. Characteristic core photographs for diatomaceous and bioturbated siltstone (Z, Zb), massive muddy sandstone (MSm), and stratified sandstone (Ss). Core sections are at the same scale (mbsf—m below seafloor). Core diameter varies due to the use of PQ, HQ, and NQ drill strings.

Interpretation

These facies were most likely deposited by pelagic to hemipelagic sedimentation from suspension settling in an ice-distal open-marine environment (Powell and Molnia, 1989; Griffith and Anderson, 1989; Svendsen et al., 1992). The presence of clasts in clusters suggests that sea ice or iceberg rafting also contributed sediment. Where the clast component is composed of granules and where it is dominated by volcanic clasts, deposition was probably predominantly from sea ice rather than from icebergs, which would carry a more polymictic clast assemblage. The relatively large biogenic and relatively small fine-grained terrigenous components in the diatomaceous siltstones (Z) are indicative of an environment with a reduced fine-grained terrigenous supply and/or a large biogenic productivity (Griffith and Anderson, 1989). In thicker units of the bioturbated siltstones (Zb), alternating bioturbated, structureless, and laminated intervals point to fluctuating sedimentation rates. In the sandy mudstones with clasts (MSm), laminated interbeds possibly indicate a periodically large terrigenous supply from turbid plumes and variations in

bottom current velocity and winnowing of fines (Svendsen et al., 1992). Evidence of iceberg rafting is more prominent in the sandy mudstones (MSm) than in the siltstone facies (Z, Zb). The minor soft-sediment deformation and gravity flow could be the result of iceberg scouring.

Stratified Facies Indicative of Proglacial Current and Turbid Plume Deposition

Three facies are characterized by distinct stratification or lamination. Differences in lithology and the type and style of stratification, however, are apparent between facies (Table 1).

(4) The stratified sandstone (Ss) facies is composed of moderately to well-sorted, fine- to medium- to locally coarse-grained sandstones that contain bedding and lamination structures (Fig. 3). Planar bedded intervals can be up to several meters thick and occur in fine, medium, and coarse sandstones, occasionally with centimeter-scale gravel-rich laminae (Fig. 3). Locally, planar bedded units fine upward or downward into thin beds of millimeter-scale interlaminated sandstones and siltstones (including pinstripe lamination). Cross-bedding occurs either as low-angle bedding or hummocky cross-stratification in fine and medium sandstones. Ripple cross-laminated and hummocky cross-stratified intervals are typically less than 1 m thick.

(5) The interstratified fine sandstone and mudstone (SMs) lithofacies is composed of centimeter- to decimeter-scale interstratified fine sandstone and mudstone (Fig. 4). Locally, internal millimeter-scale lamination structures involving abrupt transitions in particle size are typical, such as sandstone ripples with mud drapes. Individual ripple sets are between 1 and 3 cm thick. Locally, ripple sets increase and decrease in thickness over ~1-m-thick intervals, which are separated by decimeter-scale mudstone-dominated beds. Synsedimentary soft-sediment folding and loading as well as microfaulting are common. Centimeter-scale diamictite beds or clods occur, and rare outsized clasts range from coarse sand and granule to occasionally pebble size. Bioturbated horizons locally obscure the bedding structures.

(6) The interlaminated fine sandstone and siltstone (SZs) facies is characterized by millimeter- to centimeter-scale planar lamination, including pinstripe lamination of fine- to very fine-grained sandstone and siltstone (Fig. 4). Siltstone laminae are rarely cross-laminated in up to 0.5-cm-thick sets. Portions of this facies display rhythmic lamination consisting of sand-silt couplets with variations in thickness within packages of 10–20 laminae. Beds composed of

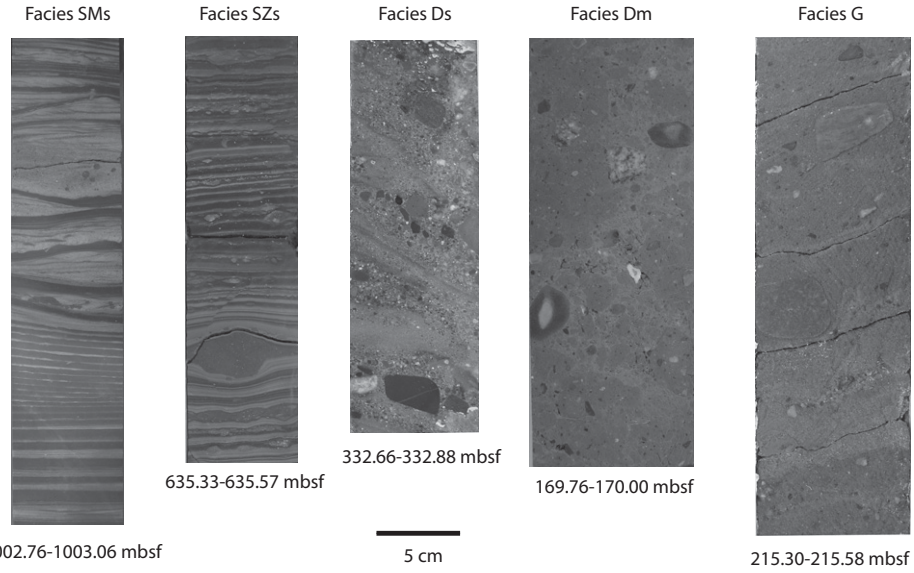

Figure 4. Characteristic core photographs for interstratified sandstone and mudstone (SMs), interlaminated sandstone and siltstone (SZs), stratified diamictite (Ds), massive diamictite (Dm), and sandy conglomerate (G). Core sections are at the same scale (mbsf—m below seafloor). Core diameter varies due to the use of PQ, HQ, and NQ drill strings.

interlaminated sandstone and siltstone display loading of sand within silt laminae, flame structures, intraformational rip-up clasts, and small clastic intrusions. Laminae can be soft-sediment deformed with microfaulting and convolute bedding. The beds generally have dispersed clasts, and clasts are observed to depress underlying laminae with draped laminae at the top. Variable proportions of the clasts consist of diamictite clods or clasts. Diamictite occurs as interbeds of up to 2 cm thick within this facies, and the proportion of diamictite generally increases downward within individual units. Locally decimeter-scale normally graded sandstone to siltstone beds are associated with this facies at its base. Unit thickness is typically <2 m, but a few units are up to 8.2 m thick.

Interpretation

For these facies, suspension sediment settling and reworking by tractional currents were the main depositional processes. Diamictite clods and dispersed clasts are interpreted as dropstones, i.e., ice-rafted debris. The stratified sandstones (Ss) may have originated from high-energy traction sedimentation by currents or waves. Where ripple cross-laminated beds occur adjacent to massive diamictites (Dm, see following), the stratified sandstones (Ss) may represent sub–ice-shelf sedimentation with ripples formed by tidal currents in the subice cavity (Domack and Harris, 1998; Hemer et al., 2007). While evidence of traction transport is dominant in the stratified sandstones (Ss), suspension settling becomes increasingly more dominant in the interstratified sandstones and mudstones (SMs) and the interlaminated sandstones and siltstones (SZs). For these latter two facies, sedimentation took place below wave base or with sea ice, allowing possible suspension settling from turbid meltwater plumes. These processes are consistent with deposition on the distal end of an ice-influenced delta or morainal bank (Lønne, 1995; Benn, 1996; Cai et al., 1997). Synsedimentary soft-sediment folding testifies to slope instability. Locally, a tidally influenced environment is suggested by the presence of mud drapes on sand ripples in the interstratified sandstone and mudstone (SMs), although these sedimentary structures can also be caused by diurnal changes in meltwater discharge. The interlaminated fine sandstones and siltstones (SZs) with diamictite clods or pellets and diamicton interbeds resemble cyclopsams and associated deposits found in temperate ice-proximal glaciomarine depositional environments off the coast of southeast Alaska (MacKiewicz et al., 1984; Cowan et al., 1997, 1999). The laminated beds there were deposited in the melting season from suspension settling, periodically interrupted by turbidity currents, which deposited the graded beds. The diamicton interbeds were deposited by ice rafting in the wintertime, when meltwater input is reduced and the residence time of icebergs in the coastal water is increased (Cowan et al., 1997, 1999).

Coarse-Grained Facies Indicative of Ice-Proximal or Iceberg-Dominated Conditions

Three coarse-grained lithofacies were also distinguished with different characteristic clast abundances, fossil content, and structure (Table 1).

(7) The stratified diamictite (Ds) lithofacies represents diamictites with wispy lamination, millimeter- to centimeter-scale sand laminae, or variations in matrix grain size on a centimeter scale (Fig. 4). The stratification is often discontinuous and soft-sediment deformed. The stratified diamictites are generally clast poor (<5% clasts) with a mud-rich or sand-rich matrix. Matrix grain size generally increases upward within individual diamictite units, from muddy at the bottom to sandy at the top. Clasts are generally of granule and pebble grade and often occur in clusters. Clast assemblages are either polymictic or rarely monomictic of volcanic origin. This facies locally has a significant volcanic or fossil component and locally grades, diffuse and gradational boundaries, into fine muddy sandstone or sandy mudstone with dispersed clasts (MSm).

(8) The massive diamictite (Dm) facies consists of structureless to clast-stratified diamictite (Fig. 4). These diamictites are clast rich or clast poor and generally have a significant sand component in the matrix. Striated and faceted clasts occur in both diamictite facies throughout the core (Fig. 5). Clast sizes are typically up to cobble grade, and clast composition is generally polymictic, although in the upper portion of the core, large proportions of intraformational mudstone clasts are present in this facies. More clast-rich diamictites sometimes have crude bedding on a decimeter to meter scale through variations in clast abundance or sand percentage of the matrix or display an alignment of the long axis of elongate clasts. Clast-poor massive diamictites locally have a significant (reworked?) fossil component. Massive diamictites locally also display pure and simple shear indicators, such as attenuated laminae, boudins, sedimentary augen (including comet structures around clasts; Fig. 6), conjugate fracture sets, or "boxwork" fracture networks with a light-colored fill. Intraclasts are common, and possible clastic intrusions up to a scale of ~1 m thick are present locally in this facies as well. Bed contacts are generally sharp.

(9) Conglomerates (G) are matrix supported or clast supported and occur generally interbedded with sandstones and occasionally with clast-rich sandy diamictites or minor siltstones (Fig. 4). Bed thickness is rarely >1 m. Clast-supported pebble-granule conglomerates occur in association with coarse sandstone and are relatively well-sorted to moderately sorted, as well as clast sorted, locally normal or reverse graded, and planar bedded or with inclined stratification. A relatively large proportion of clasts is rounded, and clearly broken, half-round clasts are occasionally present. Intraformational mudstone clasts occur occasionally as rip-up clasts at the base of individual beds of this facies. The matrix-supported pebble-cobble conglomerates are relatively poorly sorted with mud, sand, or mixed mud and sand matrix, and a variety of clast sizes. Bivalve shell fragments and serpulid tubes are present and occur in the coarsest portions of the facies. The lower contacts of this facies are generally abrupt, inclined, or loaded, except where lags of clast-supported conglomerates overlie diamictites with sharp, planar boundaries.

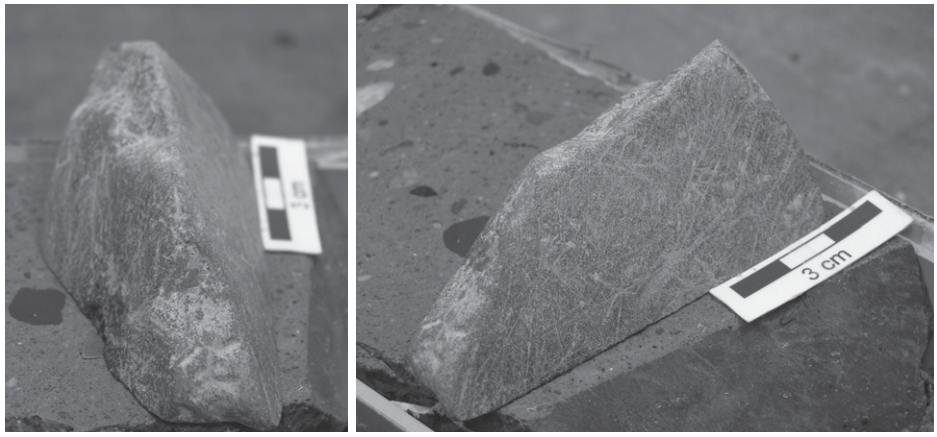

Figure 5. Striated dolerite clast at ~57.38 m below seafloor (mbsf). Scale bar has 1-cm subdivisions and is 3 cm long.

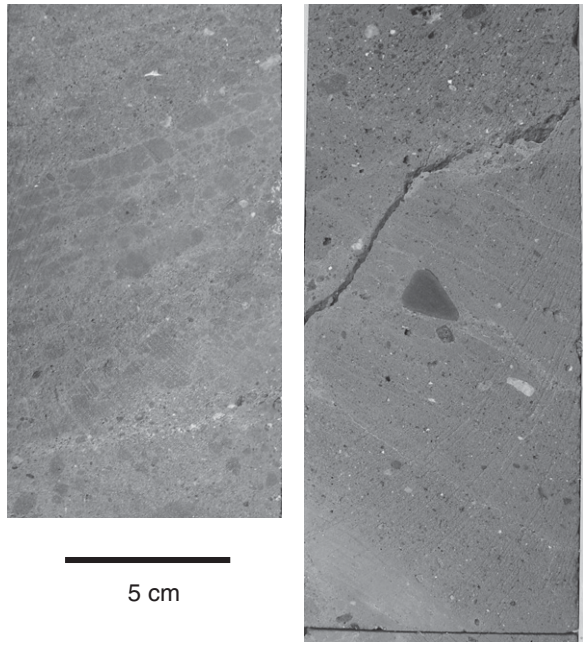

Figure 6. Evidence of soft-sediment deformation within a clast-rich diamictite at ~67 m below seafloor (mbsf; left image) and ~69 mbsf (right image), indicative of subglacial or proglacial sediment deformation in close proximity to a grounding line. Note comet structure indicative of shear deformation of matrix and rotation around clast in right image.

Interpretation

Stratified diamictites (Ds) can be formed by hemipelagic sedimentation, with significant input from icebergs, in the presence of sluggish bottom currents. In addition, both stratified (Ds) and massive diamictites (Dm) originate in subglacial or proglacial depositional environments on polar continental margins by debris melting out of the basal ice zone and subsequent deformation and mixing by subglacial and proglacial mass-wasting processes (Dowdeswell et al., 1998; Licht et al., 1999; Evans and Pudsey, 2002; Passchier et al., 2003). Deposition in an ice-proximal environment is also envisaged for the conglomerates and gravelly sandstones (G). Matrix-supported conglomerates may represent

mass-flow deposits in an ice-proximal setting, whereas thin (<1 m) beds of clast-supported conglomerates may represent transgressive lags or ice-rafted debris deposited upon ice-shelf disintegration (Evans and Pudsey, 2002). Thick units of planar-bedded, clast-supported conglomerates or units with inclined stratification are characteristic of ice-contact deltaic sediments or morainal banks (Lønne, 1995; Benn, 1996; Cai et al., 1997; Lowe and Anderson, 2002).

CHARACTERISTIC FACIES ASSOCIATIONS

Although there is significant variability in the character and vertical arrangements of facies (Fig. 7), three distinct facies associations can be recognized.

(1) A diamictite-dominated facies association (FA Dm-Ds), present in the upper ~259 m of the AND-2A core and between ~648 and 786 mbsf, ~905 and 937 mbsf, and ~1040 and 1138 mbsf, is characterized by coarsening-upward packages of laminated and cross-stratified fine sandstone (Ss), massive clast-rich diamictite (Dm), stratified clast-rich diamictite (Ds), and clast-supported conglomerates and sandstones (G). Interstratified fine sandstone and siltstone (SZs) are locally also present. The massive clast-rich diamictites have common sedimentary intraclasts and locally display shear fabrics. Six horizons, at ~65, ~135, ~239, ~659, ~763, and ~906 mbsf, show evidence of ice grounding based on the presence of macroscopic clast orientation fabrics, rotational structures, and so-called comet structures (Fig. 6). These types of structures are well documented as pure and simple shear indicators from both macroscopic and microscopic studies of ice-contact deposits (van der Meer, 1993; McCarroll and Rijsdijk, 2003).

(2) A stratified diamictite and mudstone facies association (FA Ds-Z/Zb), present between ~259 and 648 mbsf, and ~937 and 1040 mbsf, is characterized by successions of conglomerates and sandstones that are matrix supported or display inclined stratification (G), clast-poor stratified diamictites (Ds), biosiliceous mudstones (Z), massive or bioturbated clayey siltstone without clasts (Zb), and mudstone and muddy sandstone with dispersed clasts (MSm). Interstratified sandstone and mudstone (SMs) and/or ripple-laminated or parallel-laminated fine sandstone (Ss) are also common. This diamictite and mudstone facies association can be subdivided into two subassociations. Between ~937 and 1040 mbsf, siltstones have a large terrigenous component (Zb), and interstratified sandstone and mudstone (SMs) are present. In contrast, between ~259 and 648 mbsf, biosiliceous siltstones (Z) and thick units of gravel-dominated coarse-grained facies are present.

(3) A mudstone-dominated facies association (FA Zb-MSm), which is present between ~786 and 905 mbsf, consists of interbedded mudstone and muddy sandstone with dispersed clasts (MSm), and bioturbated clayey siltstone (Zb). One interbed of stratified diamictite (Ds) is present as well.

PALEOENVIRONMENTAL AND PALEOCLIMATIC INTERPRETATION OF FACIES ASSOCIATIONS

The vertical stacking patterns in facies associations result from the interplay of tectonic subsidence rates, glacial proximity, glacial basal thermal regime and ice-front geometry, sea-ice cover, glacio-isostasy, and eustasy. Throughout the early and middle Miocene, the Victoria Land basin was tectonically stable with relatively constant subsidence rates (Fielding et al., 2008a). Although changes in eustatic sea level from the Oligocene to the early Pliocene are estimated on the order of 30–60 m (Miller et al., 2005), larger changes in paleobathymetry due to self-gravitation (Bamber et al., 2009) and glacio-isostasy (Boulton, 1990) are suspected and could have resulted in a local Antarctic decrease in relative sea level during the onset of a eustatic rise and vice versa. The consequence is that facies representing the interglacial phase may have been preferentially eroded. These considerations are significant because the presence in AND-2A of wave-generated sedimentary structures in combination with trace fossils that are characteristic of inner-shelf settings requires deposition in an environment that was likely shallower than the present ~380 m water depth. This is consistent with earlier interpretations of seismic data, which suggest that the increase in water depths across McMurdo Sound was a very recent phenomenon, caused by the crustal flexure of the volcanic edifices of Ross Island ca. 1 Ma (Fielding et al., 2008a). Despite these complications, we are able to interpret the facies associations and their distribution in AND-2A as broad changes in paleoenvironmental conditions and ice extent (Fig. 8). Besides the facies characteristics themselves, the relative abundances of facies in cycles of ice-proximal to ice-distal successions are indicative of glacial regime.

Diamictite-Dominated Facies Association (FA Dm-Ds)

Diamictite-dominated facies successions are characteristic of polar continental shelves flanked by polythermal or cold ice masses (Dowdeswell et al., 1998; Evans and Pudsey, 2002). The diamictites in FA Dm-Ds are clast rich and diatom poor, and intraformational sediment clasts are common in the massive diamictites (Dm). Such clast-rich diamicts with low concentrations of diatom fragments are found beneath ice shelves away from the direct influence of currents (Domack and Harris, 1998; Evans and Pudsey, 2002; McKay et al., 2008). In addition, diamicts described from ice-shelf grounding zones are characterized by the presence of numerous intraformational sediment clasts originating from subglacial shear deformation under cold-based ice streams or cohesive debris flows near the grounding line (Domack and Harris, 1998; Khatwa and Tulaczyk, 2001; Evans and Pudsey, 2002). These diamict facies described from modern or recent ice-shelf environments bear similarities to the diamictites found in FA Dm-Ds of the AND-2A core.

The cross-stratified fine sandstones (Ss) in this facies association indicate either subice or ice-proximal sedimentation or sedimentation in a wave- and current-influenced shoreface environment, which could indicate contrasting paleoenvironmental conditions and require further study for each individual succession. Interlaminated sands and silts with cross-lamination can occur when sub–ice-shelf currents are generated by tidal pumping and thermohaline flow in a narrow cavity near the grounding line (Domack and Harris, 1998; Evans and Pudsey, 2002; Hemer et al., 2007). Although proglacial deposition cannot be entirely ruled out, the cross-laminated sands within the FA Dm-Ds unit are consistent with a sub–ice-shelf origin (Fig. 8A).

The succession of facies in FA Dm-Ds (Fig. 9) is characterized by an upward increase in clast abundance (Figs. 7 and 8), starting with stratified sandstones and siltstones (facies Ss and SZs), massive diamictites (Dm), clast-rich stratified diamictites (Ds), and conglomerates (G). The succession of facies from stratified fine-grained (Ss, SZs) to massive diamictite (Dm) marks a glacial advance. The massive clast-rich diamictites (Dm) indicate either subglacial or ice-proximal sedimentation. Following the criteria of McCarroll and Rijsdijk (2003), simple shear features in these massive diamictites can be indicative of subglacial deformation. Facies Dm, therefore, likely marks the maximum ice extent. Facies Ds is clast rich and locally fossiliferous, especially at the top of each facies succession. Therefore, Ds may signal deglaciation and a rapid transition to sub–ice-shelf or proglacial sedimentation due to ice-shelf retreat (Lowe and Anderson, 2002; Evans and Pudsey, 2002). The conglomerates and sandstones are relatively thin and generally clast supported. They could be interpreted as transgressive lags or as iceberg rafting during ice-shelf disintegration (Evans and Pudsey, 2002).

Stratified Diamictite and Mudstone Facies Association (FA Ds-Z/Zb)

The facies in this association are more characteristic of open-shelf sedimentation under meltwater-influenced settings. In fjord-shelf settings flanked by tidewater fronts (Fig. 8B), weakly laminated muds and sands with lonestones interbedded with stratified clast-rich diamictons are deposited in ice-proximal proglacial environments, followed by, upon glacial retreat, laminated and bioturbated muds deposited from surface plumes with a fluvial or fluvioglacial source (Powell and Molnia, 1989; Cowan et al., 1997; Dowdeswell et al., 1998). Conglomerates and sandstones in FA Ds-Z/Zb are typically cross-stratified, with cross-bedded conglomerates and ripple cross-laminated sandstones, which are indicative of deposition in an ice-contact delta or morainal bank setting (Lønne, 1995; Benn, 1996; Cai et al., 1997).

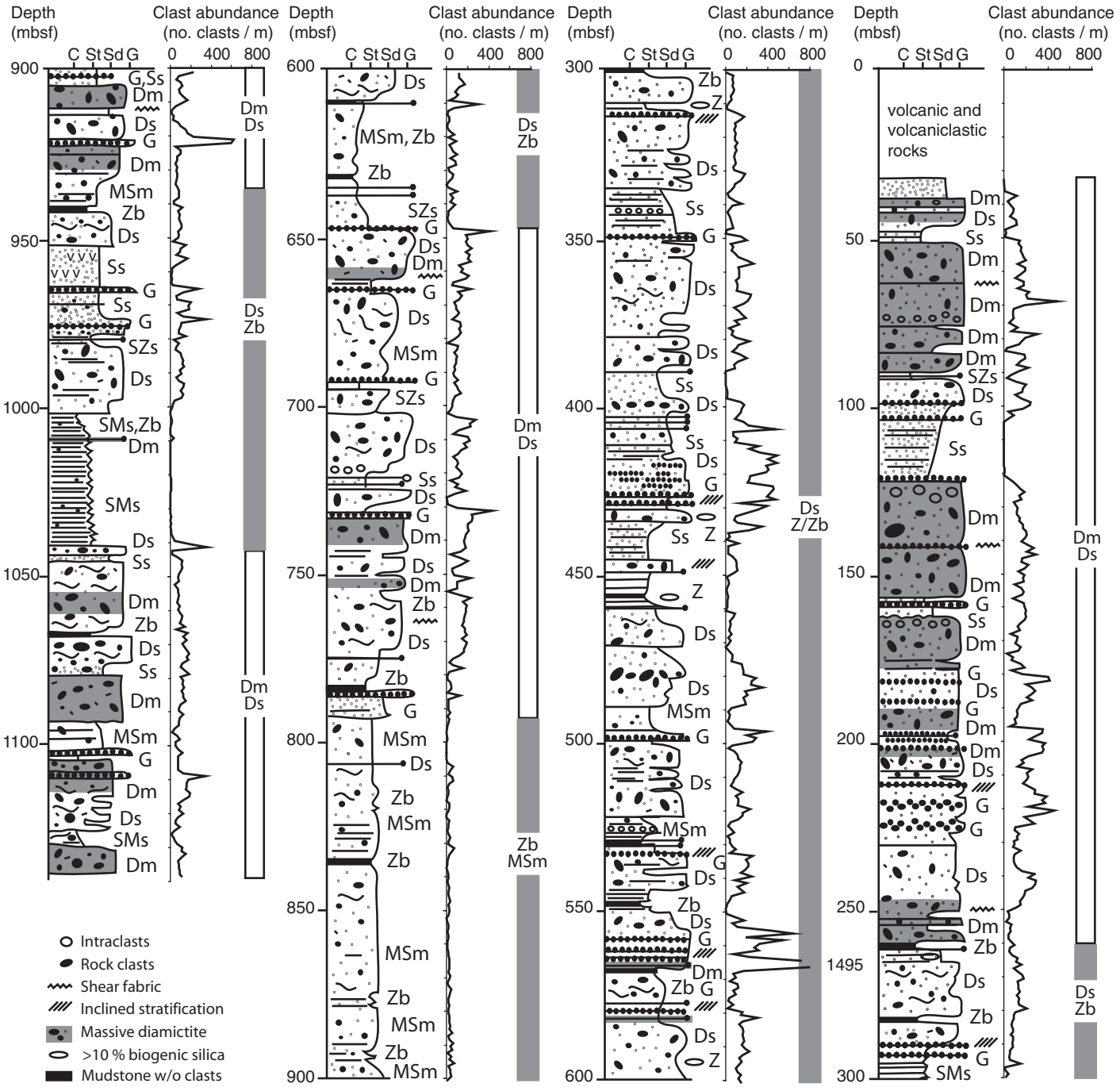

Figure 7. Graphic lithological log and clast counts per meter. Facies codes are explained in the text and in Table 1. The interval over which each facies association occurs is shown by colored bars to the right of the logs. The distribution of the diamict-dominated facies association (Dm-Ds) is indicated by the white bars, while the stratified diamictite and mudstone (Ds-Z/Zb) and mudstone-dominated facies associations (Zb-MSm) are indicated by gray bars. C—Clay; St—Silt; Sd—Sand; G—gravel.

In geological settings where rising mountains account for a large sediment supply, broad sandur plains may develop, which deposit cross-stratified to planar bedded sands and gravels (Powell and Molnia, 1989). FA Ds-Z/Zb, therefore, may represent fluctuations in the extent of outlet glaciers in the Transantarctic Mountains, which are fed by the East Antarctic Ice Sheet only, rather than a combined West and East Antarctic Ice Sheet occupying the McMurdo Sound. The dominance of conglomerates, gravelly sandstones, and diamictites associated with relatively thin units (<5 m) of bioturbated diatomaceous mudstones between ~259 and 648 mbsf (subfacies association Ds-Z), however, is possibly more indicative of a polythermal glacial regime, as indicated by comparison to modern and more recent environments in the sub-Antarctic and the Arctic (Griffith and Anderson, 1989; Svendsen et al., 1992; Etienne et al., 2003).

The succession of facies in FA Ds-Z/Zb (Fig. 9) can be explained by a glacial maximum with sedimentation on an ice-contact delta or morainal bank (G), followed by iceberg-dominated conditions (Ds), and glacial retreat (SMs through Z and Zb). The diatomaceous and weakly laminated and bioturbated mudstones (Z, Zb) may represent the glacial minimum. The overlying glacially influenced deltaic deposits (SMs) and the stratified diamictites (Ds) signal a return to ice-influenced depositional environments, associated with glacial advance.

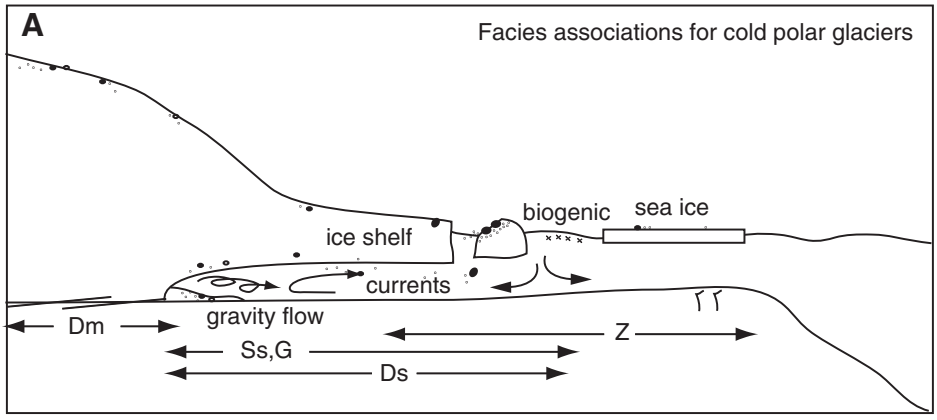

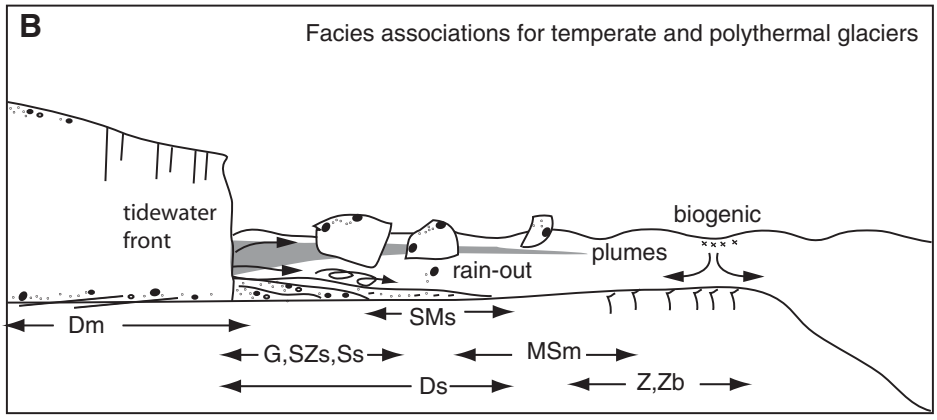

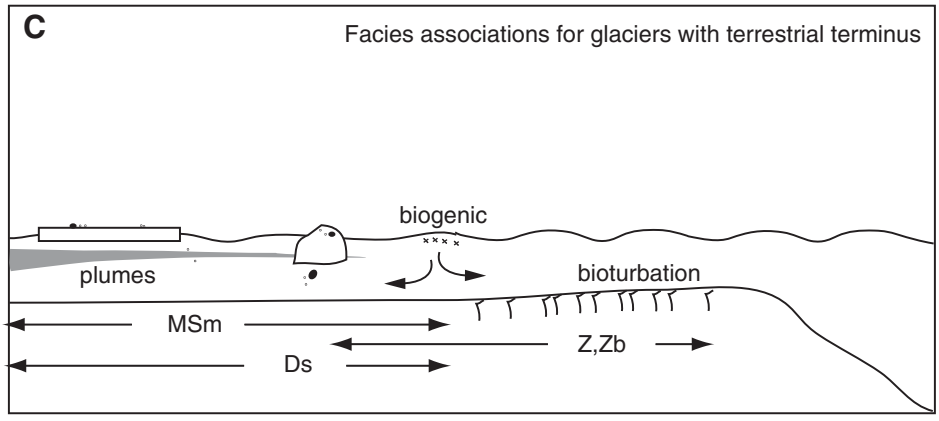

Figure 8. Facies model for the three facies associations. Facies codes are explained in the text and in Table 1. (A) Facies associations near marine-based polar ice sheets. (B) Facies associations near marine-based temperate outlet glaciers. (C) Facies associations in the marine environment near temperate ice sheets with a terrestrial terminus.

Mudstone-Dominated Facies Association (FA Zb-MSm)

The facies in association FA Zb-MSm represent hemipelagic shelf environments below wave base. Stacking patterns, consisting of alternations between bioturbated siltstones without clasts or with rare clasts (Zb) and sandy mudstones with dispersed clasts (MSm), result from small fluctuations in glacial extent during periods wherein grounding lines had retreated from McMurdo Sound (Figs. 8C and 9). Rare diamictites (Ds) suggest that iceberg production from nearby outlet glaciers was episodic. Terrigenous muds and sands with low ice-rafted debris content are typical of subarctic temperate glacial settings with high levels of precipitation and glaciers terminating on land (Griffith and Anderson, 1989). Valley glaciers in the Transantarctic Mountains, therefore, most likely retreated within the valleys and were rarely calving into McMurdo Sound. Fine-grained sediment supply, however, was as high as before (Fig. 2), indicating active erosion by nearby wet-based outlet glaciers.

Early and Middle Miocene Ice-Sheet Minima

Dynamic glacial conditions with grounding lines south of the modern position are indicated by the distribution of the stratified diamictite and mudstone facies association (Ds-Z/Zb) at ~1140–950 mbsf (20.1–19.6 Ma) and ~648–259 mbsf (ca. 17.6–15.4 Ma), which show evidence of large-amplitude cyclicity in facies associations, from open water to ice-proximal deposition (Fig. 10). The stacking patterns in FA Ds-Z/Zb result from major changes in glacial extent as witnessed by the interbedding of diamictites and conglomerates with bioturbated claystones and siltstones with or without a significant biogenic component. In contrast, the mudstone-dominated facies association

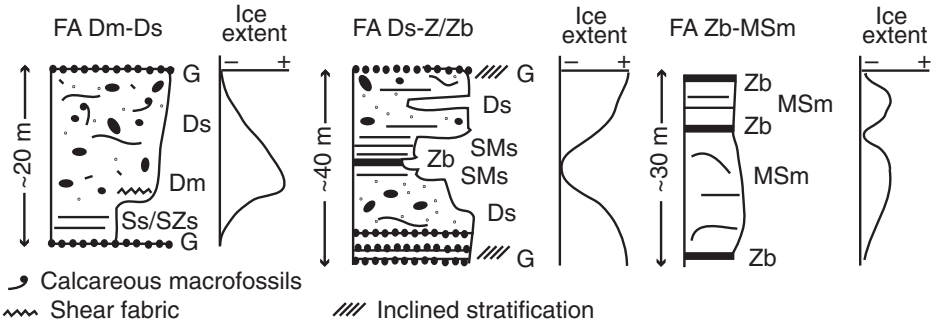

Figure 9. Genetic interpretation of stacking patterns in the facies associations with respect to variations in ice extent. Facies codes Z, Zb, MSm, Ss, SMs, SZs, Ds, Dm, and G are explained in the text and in Table 1. FA—facies association.

(Zb/MSm) at ~905–786 mbsf (19.3–18.7 Ma) lacks a significant biogenic component and is clast poor, indicative of hemipelagic deposition under high terrigenous sedimentation rates. Both facies associations resemble those of temperate and subpolar continental shelves (Figs. 8B and 8C) flanked by tidewater fronts, with the paucity of coarse-grained facies at 19.3–18.7 Ma possibly indicating a largely terrestrial margin for the Antarctic ice sheets (Cowan et al., 1997; Powell and Cooper, 2002; Griffith and Anderson, 1989).

A difference in the volumetric abundance and composition of facies between the ice-sheet minima at ~1140–937 mbsf (20.1–19.6 Ma), ~905–786 mbsf (19.3–18.7 Ma), and ~648–259 mbsf (ca. 17.6–15.4 Ma) possibly marks a difference in glacial regime. At 20.1–19.6 Ma and 19.3–18.7 Ma, large volumes of fine-grained sediments (SMs, SZs, MSm, Zb) with a paucity of clasts and a small biogenic component signal high terrigenous sedimentation rates and subordinate evidence for floating ice, indicative of temperate glacial conditions. In contrast, at ca. 17.6–15.4 Ma (~648–259 mbsf), the large volume of sandy, gravelly ice-marginal deposits, the sparse intervals of laminated mud, and the large diatom content of some distal glaciomarine mudstones are more consistent with colder and drier polythermal glacial conditions (Fig. 10).

Despite the polythermal glacial regime, glaciers were dynamic with grounding lines south of the modern position during the Miocene climatic optimum (ca. 17.6–15.4 Ma). Smear-slides and clast petrology signal the presence of a significant volcanic and biogenic component in diamictites at ~648–259 mbsf (ca. 17.6–15.4 Ma) (Panter et al., 2008). The volcanic component consists of ash derived from contemporaneous volcanoes just south of the drill site that does not appear ice-transported. Both the biogenic and the first-cycle volcanic components suggest that the diamictites were not deposited subglacially or under an ice shelf, but in a proglacial setting with open-marine conditions (Fig. 8B). Such a scenario requires a receded grounding line or an absence of the Ross Ice Shelf. The nonvolcanic clast component in the diamictites has a large proportion of striated and faceted dolerite clasts (Panter et al., 2008; Fig. 5), suggesting that ice rafting originated from valley glaciers that were actively eroding the Ferrar Group dolerite sills in the Transantarctic Mountains.

Fossiliferous strata deposited during ice-sheet and sea-ice minima and a higher biogenic productivity of diatoms, dinoflagellates, and calcareous macrofossils at ~460–431 mbsf (ca. 16.5–16.3 Ma) and ~311–296 mbsf (ca. 15.7–15.6 Ma) indicate further glacial retreat (Fig. 10). Although biogenic silica and nutrients can be advected from open water and transported to 100 km underneath an ice shelf to support suspension-feeding benthic communities, including bryozoans, sponges, and serpulid polychaetes (Riddle et al., 2007), such an environmental setting is inconsistent with the composition of the diamictites within these intervals, indicating that volcanic ash was contributed to the sediment directly through the water column or via sea ice (Fig. 10; Panter et al., 2008). The presence of >1% clasts in biosiliceous siltstones (Z) carrying up to 60% siliceous microfossils in the matrix at 296 mbsf (15.6 Ma) indicates significant ice rafting in waters of low turbidity at that time. Therefore, although the grounding lines of ice sheets had receded during the Miocene climatic optimum, complete ice-sheet collapse is less likely, except for possibly one interval of diatomite at ~311 mbsf (15.7 Ma). The paleoclimatological interpretation of that interval was discussed by Warny et al. (2009), a period when sea-surface temperatures may have been elevated. The low turbidity of the waters indicated by the biosiliceous siltstones (facies Z) in these intervals of core (16.5–16.3 and 15.7–15.6 Ma), however, is consistent with colder and drier conditions and a reduced meltwater input upon glacial retreat compared to the earlier Miocene intervals of ice retreat (20.1–19.6 Ma and 19.3–18.7 Ma).

Early and Middle Miocene Ice Growth

The distribution of the diamictite-dominated FA Dm-Ds in the core at ~1138–1040 mbsf, ~937–905 mbsf, and ~786–648 mbsf indicates that glacially dominated conditions with only brief periods of ice retreat occurred in McMurdo Sound at 20.2–20.1 Ma, 19.6–19.3 Ma, 18.7–17.6 Ma, and later than 15.4 Ma (Fig. 10). Shear fabrics in diamictites at and below ~906, ~763, and ~659 mbsf (Fig. 7) indicate that the ice sheet became grounded on the shelf near the drill site at ca. 19.4 Ma, ca. 18.6 Ma, and ca. 17.6 Ma, indicating larger than modern ice volumes for these times.

Major ice advance in AND-2A at ca. 18.7–17.6 Ma overlaps with a core interval in CRP-1 showing conclusive evidence of subglacial shear deformation at ~79 mbsf (ca. 17.6 Ma) within an interval characterized by a glacial weathering regime, correlative to the Mi-1b marine isotopic event (Passchier et al., 1998; Passchier and Krissek, 2008). The presence of coarsening-upward sequences of coarse-grained facies, intraclasts, and a general lack of meltwater-related facies at ~786–659 mbsf in AND-2A (Fig. 7) suggests that the glacial regime may have been cold with the presence of ice shelves, similar to the polar ice-sheet conditions of today (Evans and Pudsey, 2002), although it cannot be entirely ruled out that meltwater-related facies were preferentially removed by erosion.

The oldest middle Miocene ice grounding event near the drill site is recognized by deformed massive diamictites present at ~240 mbsf (ca. 14.7 Ma). Upward from this stratigraphic level (younger), the cores are characterized by abundant massive diamictites without a significant first-cycle volcanic ash or fine-grained biogenic component (Panter et al., 2008, p. 37). Shear fabrics in the diamictites indicate that the ice sheet became grounded on the shelf multiple times, indicating grounding lines extending beyond the present position starting at ca. 14.7 Ma. The presence of possible hummocky cross-stratification in the upper portion of AND-2A, however, suggests that the coast may have been ice-free during brief periods after ca. 14.7 Ma, which is documented in more detail in the record of the AND-1B site (Fig. 1; McKay et al., 2009; Naish et al., 2009).

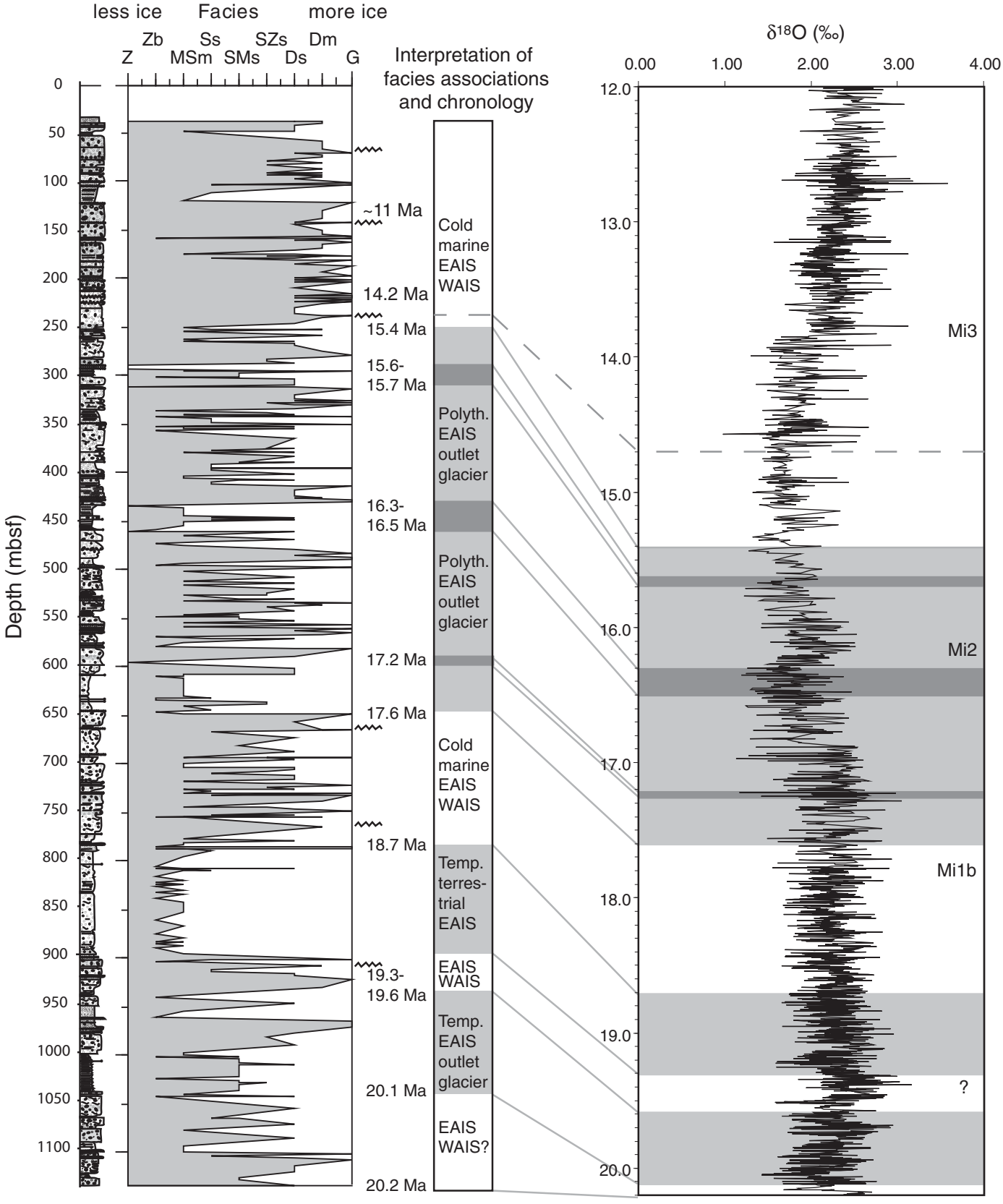

Figure 10. Lithological log (mbsf—m below seafloor), facies distribution, chronology, and paleoenvironmental interpretation for AND-2A compared to oxygen isotope curve of Zachos et al. (2008). Facies codes correspond to those in Table 1. Mi—Miocene isotope excursions according to Miller et al. (1991).

Paleoclimatic Implications

There is generally good agreement between the findings of this study and ice-volume reconstructions based on far-field records (Fig. 10). The ice-sheet and sea-ice minima at 16.5–16.3 and 15.7–15.6 Ma recorded in AND-2A correspond to periods of high-amplitude global sea-level fluctuations and ice-volume reduction as deduced from the stratigraphy of passive continental margins, and oxygen isotope and Mg/Ca measurements on benthic foraminifera (Miller et al., 1991, 1996; Lear et al., 2000; Billups and Schrag, 2002; Shevenell et al., 2004; Zachos et al., 2008). In comparison with the Zachos et al. (2008) oxygen isotope record, glacially dominated intervals between 20.2 and 17.6 Ma in AND-2A generally coincide with increased $\delta^{18}O$ values. The facies distribution of AND-2A, however, shows that the early and middle Miocene ice sheets were periodically larger than today's ice sheets. The 18.7–17.6 Ma period of glacial intensification and ice growth in AND-2A can be tentatively correlated to the Mi-1b glacial event of Miller et al. (1991). On the other hand, the Mi-2 event of Miller et al. (1991) is recognized as ice-contact deltaic deposits from advanced East Antarctic outlet glaciers at ~431–412 mbsf (ca. 16.3–16.2 Ma) in AND-2A, without evidence of a large ice sheet and ice shelves overriding the drill site.

Tills in the Dry Valleys indicate a transition to dry-based glacial conditions corresponding to a decrease in surface temperatures as early as ca. 15 Ma, but no later than ca. 13.94 Ma (Lewis et al., 2007). The record from AND-2A, however, suggests that cold glaciers with ice shelves existed periodically from at least 18.7 Ma onward, with a return to dynamic polythermal glaciers during the Miocene climatic optimum (17.6–15.4 Ma). Glacial intensification at ca. 15.4 Ma identified in AND-2A coincides with the onset of major fluctuations in Mg/Ca-based bottom-water temperatures and strongly fluctuating Mg/Ca-based sea-surface temperatures in the Southern Ocean (Billups and Schrag, 2002; Shevenell et al., 2004, 2008). The large isotope shift at 13.9–13.8 Ma in $\delta^{18}O$ records is generally attributed to major ice growth in Antarctica, concomitant with bottom-water cooling (Holbourn et al., 2005). In AND-2A, however, major ice advance at the middle Miocene climate transition to an ice extent beyond the modern grounding line positions began at ca. 14.7 Ma, around ~1 m.y. earlier. Further, at Ocean Drilling Program Site 1165 off Prydz Bay, lower sedimentation rates, an increase in ice-rafted debris, and an increase in shelf-derived foraminifera and glauconite suggest that cooling and ice advance onto the shelf took place at ca. 14.3 Ma (Florindo et al., 2003). These results are in agreement with evidence from Mg/Ca-temperature–corrected $\delta^{18}O$ records from the Southern Ocean, which suggest that ice growth was stepwise between 15 and 13.8 Ma (Shevenell et al., 2008). If ice-sheet advance onto the shelf had occurred by ca. 14.7–14.3 Ma, it would have largely preceded the cooling of sea-surface temperatures in the Southern Ocean (14.2–13.8 Ma) (Shevenell et al., 2004). The latter is more consistent with modeling studies, which show that the formation of a grounded ice sheet on the shelf would be required to significantly cool the surface of the ocean (DeConto et al., 2007).

CONCLUSIONS

The early and middle Miocene strata drilled in AND-2A produce a unique record of Antarctic ice-sheet advance and retreat. Three facies associations are recognized, which record changes in ice extent and paleoenvironments within the Ross Sea embayment.

(1) A diamictite-dominated facies association (Dm-Ds) is characterized by the presence of massive diamictites with pure and simple shear deformation, indicative of grounding of an ice sheet on the shelf. This facies association is found in core dated at 20.2–20.1 Ma, 19.6–19.3 Ma, 18.7–17.6 Ma, and younger than 15.4 Ma. A cold glacial regime with ice shelves is envisioned for the diamictite-dominated successions through the early and middle Miocene.

(2) A stratified diamictite-mudstone facies association (Ds-Z/Zb) is characterized as interbedded biosiliceous mudstones, mudstones with clasts, interlaminated sandstones and mudstones with clasts, stratified diamictites, and conglomerates, indicative of fluctuations in the extent of tidewater glaciers draining the East Antarctic Ice Sheet. This facies association is found in core dated ca. 20.1–19.6 Ma and ca. 17.6–15.4 Ma.

(3) A mudstone-dominated facies association (MSm-Zb) at 19.3–18.7 Ma generally lacks diamictites and represents ice sheets at their minimum extent, with predominantly meltwater plume deposition and minor ice rafting. This facies association is typical of a temperate glacial regime with glaciers terminating on land.

Although a temperate glacial regime is indicated for glacial minima at 20.1–19.6 and 19.3–18.7 Ma, decreased terrigenous supply in interglacials and deposition of gravel-rich deposits during glacials suggest that it may have been colder and drier with polythermal ice conditions during the Miocene climatic optimum (17.6–15.4 Ma).

The facies distribution in AND-2A can be related to shifts in oxygen isotope ratios. On a broad scale, ice-retreat phases generally coincide with minima in the $\delta^{18}O$ records, and ice advances generally correlate to $\delta^{18}O$ shifts to higher values. However, discrepancies were also identified. Ice advance on the Antarctic continental margin, to an ice sheet larger than modern proportions, at ca. 14.7–14.3 Ma preceded the cooling event and the major oxygen isotope shift of the middle Miocene climate transition (Shevenell et al., 2004; Holbourn et al., 2005) and is more consistent with a stepwise pattern of ice growth (Shevenell et al., 2008). This study demonstrates that the mechanisms that cause major changes in ocean chemistry and the paleoclimate of the Southern Ocean are poorly understood from far-field records alone. Further reconstructions of the Antarctic ice sheets across major climate transitions are, therefore, necessary to determine the controls on fluctuations in stable isotope proxies.

ACKNOWLEDGMENTS

This material is based upon work supported by the National Science Foundation under Cooperative Agreement 0342484 through subawards administered by the Antarctic Geologic Drilling (ANDRILL) Science Management Office at the University of Nebraska–Lincoln as part of the ANDRILL U.S. Science Support Program. Any opinions, findings, and conclusions or recommendations expressed in this material are those of the authors and do not necessarily reflect the views of the National Science Foundation.

The ANDRILL Program is a multinational collaboration among the Antarctic programs of Germany, Italy, New Zealand, and the United States. Antarctica New Zealand is the project operator and developed the drilling system in collaboration with Alex Pyne at Victoria University of Wellington and Webster Drilling and Exploration. The U.S. Antarctic Program (USAP) and Raytheon Polar Services Corporation (RPSC) supported the science team at McMurdo Station and in the Crary Science and Engineering Laboratory, while Antarctica New Zealand supported the drilling team at Scott Base. Scientific studies for the ANDRILL Program are jointly supported by the U.S. National Science Foundation, New Zealand Foundation for Research, the Italian Antarctic Research Program, the German Science Foundation, and the Alfred Wegener Institute.

Ellen A. Cowan and Michael J. Hambrey are thanked for helpful reviews that significantly improved the paper.

REFERENCES CITED

Acton, G., Florindo, F., Jovane, L., Lum, B., Ohneiser, C., Sagnotti, L., Strada, E., Verosub, K.L., Wilson, G.S., and the ANDRILL-SMS Science Team, 2008, Preliminary integrated chronostratigraphy of the AND-2A Core, ANDRILL Southern McMurdo Sound Project, Antarctica, *in* Harwood, D.M., Florindo, F., Talarico, F., and Levy, R.H., eds., Studies from the ANDRILL, Southern McMurdo Sound Project, Antarctica: Terra Antartica, v. 15, p. 211–220.

Bamber, J., Riva, R.E.M., Vermeersen, B.L.A., and LeBrocq, A.M., 2009, Reassessment of the potential sea-level rise from a collapse of the West Antarctic Ice Sheet: Science, v. 324, no. 5929, p. 901–903, doi: 10.1126/science.1169335.

Barrett, P.J., 2007, Cenozoic climate and sea level history from glacimarine strata off the Victoria Land coast, Cape Roberts Project, Antarctica, *in* Hambrey, M.J., Christoffersen, P., Glasser, N.F., and Hubbart, B., eds., Glacial Processes and Products: International Association of Sedimentologists Special Publication 39, p. 259–287.

Barrett, P.J., and Hambrey, M.J., 1992, Plio-Pleistocene sedimentation in Ferrar Fjord, Antarctica: Sedimentology, v. 39, p. 109–123, doi: 10.1111/j.1365-3091.1992.tb01025.x.

Benn, D., 1996, Subglacial and subaqueous processes near a glacier grounding line: Sedimentological evidence from a former ice-dammed lake, Achnasheen Scotland: Boreas, v. 25, p. 23–36, doi: 10.1111/j.1502-3885.1996.tb00832.x.

Billups, K., and Schrag, D.P., 2002, Paleotemperatures and ice volume of the past 27 Myr revisited with paired Mg/Ca and $^{18}O/^{16}O$ measurements on benthic foraminifera: Paleoceanography, v. 17, no. 1, PA000567, doi: 10.1029/2000PA000567.

Boulton, G.S., 1990, Sedimentary and sea level changes during glacial cycles and their control on glacimarine facies architecture, *in* Dowdeswell, J.A., and Scourse, J.D., eds., Glaciomarine Environments: Processes and Sediments: Geological Society of London Special Publication 53, p. 15–52.

Cai, J., Powell, R.D., Cowan, E.A., and Carlson, P.R., 1997, Lithofacies and seismic-reflection interpretation of temperate glacimarine sedimentation in Tarr Inlet, Glacier Bay, Alaska: Marine Geology, v. 143, p. 5–37, doi: 10.1016/S0025-3227(97)00088-1.

Cowan, E.A., Cai, J., Powell, R.D., Clark, J.D., and Pitcher, J.N., 1997, Temperate glacimarine varves: An example of Disenchantment Bay, southern Alaska: Journal of Sedimentary Research, v. 67, p. 536–549.

Cowan, E.A., Seramur, K.C., Cai, J., and Powell, R.D., 1999, Cyclic sedimentation produced by fluctuation in meltwater discharge, tides, and marine productivity in an Alaskan fjord: Sedimentology, v. 46, p. 1109–1126, doi: 10.1046/j.1365-3091.1999.00267.x.

DeConto, R.M., and Pollard, D., 2003, Rapid Cenozoic glaciation of Antarctica induced by declining atmospheric CO_2: Nature, v. 421, p. 245–249, doi: 10.1038/nature01290.

DeConto, R., Pollard, D., and Harwood, D., 2007, Sea ice feedback and Cenozoic evolution of Antarctic climate and ice sheets: Paleoceanography, v. 22, p. PA3214, doi: 10.1029/2006PA001350.

Del Carlo, P., Panter, K.S., Bassett, K., Bracciali, L., Di Vincenzo, G., and Rocchi, S., 2009, The upper lithostratigraphic unit of ANDRILL AND-2A core (Southern McMurdo Sound, Antarctica): Local volcanic sources, paleoenvironmental implications and subsidence in the western Victoria Land Basin: Global and Planetary Change, v. 69, p. 142–161, doi: 10.1016/j.gloplacha.2009.09.002.

Di Vincenzo, G., Bracciali, L., Del Carlo, P., Panter, K., and Rocchi, S., 2010, $^{40}Ar/^{39}Ar$ laser dating of volcanogenic products from the AND-2A core (ANDRILL Southern McMurdo Sound Project, Antarctica): Bulletin of Volcanology, v. 72, p. 487–505, doi: 10.1007/s00445-009-0337-z.

Domack, E.W., and Harris, P., 1998, A new depositional model for ice shelves based upon sediment cores from the Ross Sea and the MacRobertson shelf, Antarctica: Annals of Glaciology, v. 27, p. 281–284.

Domack, E.W., Duran, D., Leventer, A., Ishman, S., Doane, S., McCallum, S., Amblas, D., Ring, J., Gilbert, R., and Prentice, M., 2005, Stability of the Larsen B ice shelf on the Antarctic Peninsula during the Holocene Epoch: Nature, v. 436, p. 681–685, doi: 10.1038/nature03908.

Dowdeswell, J.A., Elverhøi, A., and Spielhagen, R., 1998, Glacimarine sedimentary processes and facies on the polar North Atlantic margins: Quaternary Science Reviews, v. 17, p. 243–272, doi: 10.1016/S0277-3791(97)00071-1.

Ehrmann, W., Setti, M., and Marinoni, L., 2005, Clay minerals in Cenozoic sediments off Cape Roberts (McMurdo Sound, Antarctica) reveal palaeoclimatic history: Palaeogeography, Palaeoclimatology, Palaeoecology, v. 229, p. 187–211, doi: 10.1016/j.palaeo.2005.06.022.

Etienne, J.L., Glasser, N.F., and Hambrey, M.J., 2003, Proglacial sediment-landform associations of a polythermal glacier: Storglaciären, northern Sweden: Geografiska Annaler, v. 85, no. A, p. 149–164.

Evans, J., and Pudsey, C.J., 2002, Sedimentation associated with Antarctic Peninsula ice shelves: Implications for palaeoenvironmental reconstructions of glacimarine sediments: Journal of the Geological Society of London, v. 159, no. 3, p. 233–237, doi: 10.1144/0016-764901-125.

Fielding, C.R., Whittaker, J., Henrys, S.A., Wilson, T.J., and Naish, T.R., 2008a, Seismic facies and stratigraphy of the Cenozoic succession in McMurdo Sound, Antarctica: Implications for tectonic, climatic and glacial history: Palaeogeography, Palaeoclimatology, Palaeoecology, v. 260, p. 8–29, doi: 10.1016/j.palaeo.2007.08.016.

Fielding, C.R., Atkins, C.B., Bassett, K.N., Browne, G.H., Dunbar, G.B., Field, B.D., Frank, T.D., Krissek, L.A., Panter, K., Passchier, S., Pekar, S.F., and the ANDRILL-SMS Science Team, 2008b, Sedimentology and stratigraphy of the AND-2A core, ANDRILL Southern McMurdo Sound, Project, Antarctica: Terra Antartica, v. 15, p. 77–112.

Florindo, F., Bohaty, S.M., Erwin, P.S., Richter, C., Roberts, A.P., Whalen, P.A., and Whitehead, J.M., 2003, Magnetobiostratigraphic chronology and palaeoenvironmental history of Cenozoic sequences from ODP Sites 1165 and 1166, Prydz Bay, Antarctica: Palaeogeography, Palaeoclimatology, Palaeoecology, v. 198, p. 69–100, doi: 10.1016/S0031-0182(03)00395-X.

Griffith, T.W., and Anderson, J.B., 1989, Climatic control of sedimentation in bays and fjords of the northern Antarctic Peninsula: Marine Geology, v. 85, p. 181–204, doi: 10.1016/0025-3227(89)90153-9.

Hambrey, M.J., and McKelvey, B.C., 2000, Major Neogene fluctuations of the East Antarctic Ice Sheet: Stratigraphic evidence from the Lambert glacier region: Geology, v. 28, p. 887–890, doi: 10.1130/0091-7613(2000)28<887:MNFOTE>2.0.CO;2.

Hambrey, M.J., Bennett, M.R., Dowdeswell, J.A., Glasser, N.F., and Huddard, D., 1999, Debris entrainment and transfer in polythermal valley glaciers: Journal of Glaciology, v. 149, no. 45, p. 69–86.

Harwood, D.M., 1986, Diatom Biostratigraphy and Paleoecology with a Cenozoic History of Antarctic Ice Sheets [Ph.D. thesis]: Columbus, Ohio, The Ohio State University, 592 p.

Harwood, D.M., and Webb, P.-N., 1998, Glacial transport of diatoms in the Antarctic Sirius Group: Pliocene refrigerator: GSA Today, v. 8, no. 4, p. 1–8.

Hemer, M.A., Post, A.L., O'Brien, P.E., Craven, M., Truswell, E.M., Roberts, D., and Harris, P.T., 2007, Sedimentological signatures of the sub–Amery Ice Shelf circulation: Antarctic Science, v. 19, p. 497–506, doi: 10.1017/S0954102007000697.

Holbourn, A., Kuhnt, W., Schulz, M., and Erlenkeuser, H., 2005, Impacts of orbital forcing and atmospheric carbon dioxide on Miocene ice-sheet expansion: Nature, v. 438, p. 483–487, doi: 10.1038/nature04123.

Ishman, S.E., and Rieck, H.J., 1992, A late Neogene Antarctic glacio-eustatic record, Victoria Land Basin margin, Antarctica: Antarctic Research Series, v. 56, p. 327–348.

Joseph, L.H., Rea, D.K., van der Pluijm, B.A., and Gleason, D.A., 2002, Antarctic environmental variability since the late Miocene: ODP Site 745, the East Kerguelen sediment drift: Earth and Planetary Science Letters, v. 201, p. 127–142, doi: 10.1016/S0012-821X(02)00661-1.

Khatwa, A., and Tulaczyk, S., 2001, Microstructural interpretations of modern and Pleistocene subglacially deformed sediments: The relative role of parent material and subglacial processes: Journal of Quaternary Science, v. 16, no. 6, p. 507–517, doi: 10.1002/jqs.609.

Lear, C.H., Elderfield, H., and Wilson, P.A., 2000, Cenozoic deep-sea temperatures and global ice volumes from Mg/Ca in benthic foraminiferal calcite: Science, v. 287, p. 269–272, doi: 10.1126/science.287.5451.269.

Lear, C.H., Rosenthal, Y., Coxall, H.K., and Wilson, P.A., 2004, Late Eocene to early Miocene ice-sheet dynamics and the global carbon cycle: Paleoceanography, v. 19, no. 4, p. PA4015, doi: 10.1029/2004PA001039.

Lear, C.H., Bailey, T.R., Pearson, P.N., Coxall, H.K., and Rosenthal, Y., 2008, Cooling and ice growth across the Eocene-Oligocene transition: Geology, v. 36, p. 251–254, doi: 10.1130/G24584A.1.

Lewis, A.R., Marchant, D.R., Ashworth, A.C., Hemming, S.R., and Machlus, M.L., 2007, Major middle Miocene global climate change: Evidence from East Antarctica and the Transantarctic Mountains: Geological Society of America Bulletin, v. 119, p. 1449–1461.

Licht, K.J., Dunbar, N.W., Andrews, J.T., and Jennings, A.E., 1999, Distinguishing subglacial till and glacial marine diamictons in the western Ross Sea, Antarctica: Implications for a Last Glacial Maximum grounding line: Geological Society of America Bulletin, v. 111, p. 91–103, doi: 10.1130/0016-7606(1999)111<0091:DSTAGM>2.3.CO;2.

Lowe, A.L., and Anderson, J.B., 2002, Late Quaternary advance and retreat of the West Antarctic Ice Sheet in Pine Island Bay, Antarctica: Quaternary Science Reviews, v. 21, p. 1879–1897, doi: 10.1016/S0277-3791(02)00006-9.

Lønne, I., 1995, Sedimentary facies and depositional architecture of ice-contact glaciomarine systems: Sedimentary Geology, v. 98, p. 13–43, doi: 10.1016/0037-0738(95)00025-4.

MacKiewicz, N.E., Powell, R.D., Carlson, P.R., and Molnia, B.F., 1984, Interlaminated ice-proximal glacimarine sediments in Muir Inlet, Alaska: Marine Geology, v. 57, no. 1–4, p. 113–147, doi: 10.1016/0025-3227(84)90197-X.

Marchant, D.R., Denton, G.H., Sugden, D.E., and Swisher, C.C., III, 1993, Miocene glacial stratigraphy and landscape evolution of the western Asgard Range, Antarctica: Geografiska Annaler, v. 75A, no. 4, p. 303–330, doi: 10.2307/521205.

McCarroll, D., and Rijsdijk, K., 2003, Deformation styles as a key for unlocking glacial depositional environments: Journal of Quaternary Science, v. 18, p. 473–489, doi: 10.1002/jqs.780.

McKay, R.M., Dunbar, G.B., Naish, T., Barrett, P.J., Carter, L., and Harper, M., 2008, Retreat history of the Ross Ice Sheet (Shelf) since the Last Glacial Maximum from deep-basin sediment cores around Ross Island: Palaeogeography, Palaeoclimatology, Palaeoecology, v. 260, p. 245–261, doi: 10.1016/j.palaeo.2007.08.015.

McKay, R.M., Browne, G., Carter, L., Cowan, E., Dunbar, G., Krissek, L., Naish, T., Powell, R., Reed, J., Talarico, F., and Wilch, T., 2009, The stratigraphic signature of the late Cenozoic Antarctica Ice Sheets in the Ross Embayments: Geological Society of America Bulletin, v. 121, p. 1537–1561, doi: 10.1130/B26540.1.

McKelvey, B.C., 1981, The lithologic logs of DVDP cores 10 and 11, eastern Taylor Valley, *in* McGinnis, L.D., ed., Dry Valley Drilling Project: Antarctic Research Series: Washington, D.C., American Geophysical Union, p. 63–94.

McKelvey, B.C., 1982, Late Cenozoic marine and terrestrial glacial sedimentation in eastern Taylor Valley, Southern Victoria Land, *in* Craddock, C., ed., Proceedings of the Third Symposium on Antarctic Geology and Geophysics: Madison, Wisconsin, The University of Wisconsin Press, p. 1109–1116.

Miller, K.G., Wright, J.D., and Fairbanks, R.G., 1991, Unlocking the ice house: Oligocene-Miocene oxygen isotopes, eustasy, and margin erosion: Journal of Geophysical Research, v. 96, p. 6829–6848, doi: 10.1029/90JB02015.

Miller, K.G., Mountain, G.S., the Leg 150 Shipboard Party, and Members of the New Jersey Coastal Plain Drilling Project, 1996, Drilling and dating New Jersey Oligocene-Miocene sequences: Ice volume, global sea level, and Exxon records: Science, v. 271, p. 1092–1094.

Miller, K.G., Kominz, M.A., Browning, J.V., Wright, J.D., Mountain, G.S., Katz, M.E., Sugarman, P.J., Cramer, B.S., Christie-Blick, N., and Pekar, S.F., 2005, The Phanerozoic record of global sea-level change: Science, v. 310, p. 1293–1298, doi: 10.1126/science.1116412.

Moncrieff, A.C.M., 1989, Classification of poorly-sorted sedimentary rocks: Sedimentary Geology, v. 65, p. 191–194, doi: 10.1016/0037-0738(89)90015-8.

Naish, T.R., and 32 others, 2001, Orbitally induced oscillations in the East Antarctic Ice Sheet at the Oligocene/

Miocene boundary: Nature, v. 413, p. 719–723, doi: 10.1038/35099534.
Naish, T., and 55 others, 2009, Obliquity-paced Pliocene West Antarctic Ice Sheet oscillations: Nature, v. 458, p. 322–328, doi: 10.1038/nature07867.
Ó Cofaigh, C., and Dowdeswell, J.A., 2001, Laminated sediments in glacimarine environments: Diagnostic criteria for their interpretation: Quaternary Science Reviews, v. 20, p. 1411–1436.
Ó Cofaigh, C., Dowdeswell, J.A., and Grobe, H., 2001, Holocene glacimarine sedimentation, inner Scoresby Sund, East Greenland: The influence of fast-flowing ice-sheet outlet glaciers: Marine Geology, v. 175, p. 103–129.
Pagani, M., Zachos, J., Freeman, K.H., Bohaty, S., and Tipple, B., 2005, Marked change in atmospheric carbon dioxide concentrations during the Oligocene: Science, v. 309, p. 600–603, doi: 10.1126/science.1110063.
Panter, K.S., Talarico, F., Bassett, K., Del Carlo, P., Field, B., Frank, T., Hoffman, S., Kuhn, G., Reichelt, L., Sandroni, S., Tavini, M., Bracciali, L., Cornamusini, G., von Eynatten, H., and Rocchi, R., 2008, Petrologic and geochemical composition of the AND-2A core, ANDRILL Southern McMurdo Sound Project, Antarctica, *in* Harwood, D.M., Florindo, F., Talarico, F., and Levy, R.H., eds., Studies from the ANDRILL, Southern McMurdo Sound Project, Antarctica: Terra Antarctica, v. 15, p. 147–192.
Passchier, S., and Krissek, L.A., 2008, Oligocene–Miocene Antarctic continental weathering record and paleoclimatic implications, Cape Roberts Drilling Project, Ross Sea, Antarctica: Palaeogeography, Palaeoclimatology, Palaeoecology, v. 260, p. 30–40, doi: 10.1016/j.palaeo.2007.08.012.
Passchier, S., Wilson, T.J., and Paulsen, T.S., 1998, Origin of breccias in the CRP-1 core: Terra Antartica, v. 5, no. 3, p. 401–409.
Passchier, S., O'Brien, P.E., Damuth, J.E., Januszczack, N., Handwerger, D.A., and Whitehead, J.M., 2003, Pliocene-Pleistocene glaciomarine sedimentation in eastern Prydz Bay and development of the Prydz trough-mouth fan, ODP Sites 1166 and 1167, East Antarctica: Marine Geology, v. 199, p. 179–305.
Pekar, S.F., and DeConto, R.M., 2006, High-resolution ice-volume estimates for the early Miocene: Evidence for a dynamic ice sheet in Antarctica: Palaeogeography, Palaeoclimatology, Palaeoecology, v. 231, p. 101–109, doi: 10.1016/j.palaeo.2005.07.027.
Powell, R.D., 1981, Sedimentation conditions in Taylor Valley, Antarctica, inferred from textural analysis of DVDP cores, *in* McGinnis, L.D., ed., Dry Valley Drilling Project: Antarctic Research Series: Washington, D.C., American Geophysical Union, p. 331–349.
Powell, R.D., and Cooper, J.M., 2002, A glacial sequence stratigraphic model for temperate, glaciated continental shelves, *in* Dowdeswell, J.A., and Ó Cofaigh, C., eds., Glacier-Influenced Sedimentation on High-Latitude Continental Margins: Geological Society of London Special Publication 203, p. 215–244.
Powell, R.D., and Molnia, B.F., 1989, Glacimarine sedimentary processes, facies and morphology of the south-southeast Alaska shelf and fjords: Marine Geology, v. 85, p. 359–390, doi: 10.1016/0025-3227(89)90160-6.
Prentice, M.L., Bockheim, J.G., Wilson, S.C., Burckle, L.H., Hodell, D.A., Schlüchter, C., and Kellogg, D.E., 1993, Late Neogene Antarctic glacial history: Evidence from Central Wright Valley, *in* Kennett, J.P., and Warnke, D.A., eds., The Antarctic Paleoenvironment: A Perspective on Global Change, Part 2: Antarctic Research Series: Washington, D.C., American Geophysical Union, p. 207–250.
Rebesco, M., Camerlenghi, A., Geletti, R., and Canals, M., 2006, Margin architecture reveals the transition to the modern Antarctic ice sheet ca. 3 Ma: Geology, v. 34, no. 4, p. 301–304, doi: 10.1130/G22000.1.
Riddle, M.J., Craven, M., Goldsworthy, P.M., and Carsey, F., 2007, A diverse benthic assemblage 100 km from open water under the Amery Ice Shelf, Antarctica: Paleoceanography, v. 22, p. PA1204, doi: 10.1029/2006PA001327.
Shevenell, A.E., Kennett, J.P., and Lea, D.W., 2004, Middle Miocene Southern Ocean cooling and Antarctic cryosphere expansion: Science, v. 305, p. 1766–1770, doi: 10.1126/science.1100061.
Shevenell, A.E., Kennett, J.P., and Lea, D.W., 2008, Middle Miocene ice sheet dynamics, deep-sea temperatures, and carbon cycling: A Southern Ocean perspective: Geochemistry, Geophysics, Geosystems, v. 9, no. 2, Q02006, p. 1–14.
Sugden, D., and Denton, G., 2004, Cenozoic landscape evolution of the Convoy Range to Mackay Glacier area, Transantarctic Mountains: Onshore to offshore synthesis: Geological Society of America Bulletin, v. 116, p. 840–857, doi: 10.1130/B25356.1.
Svendsen, J.I., Mangerud, J., Elverhøi, A., Solheim, A., and Schüttenhelm, R.T.E., 1992, The late Weichselian glacial maximum on western Spitsbergen inferred from offshore sediment cores: Marine Geology, v. 104, p. 1–17, doi: 10.1016/0025-3227(92)90081-R.
Tripati, A.K., Roberts, C.D., and Eagle, R.A., 2009, Coupling of CO_2 and ice sheet stability over major climate transitions of the last 20 million years: Science, v. 326, no. 5958, p. 1394–1397, doi: 10.1126/science.1178296.
van der Meer, J.J.M., 1993, Microscopic evidence of subglacial deformation: Quaternary Science Reviews, v. 12, p. 553–587, doi: 10.1016/0277-3791(93)90069-X.
Warny, S., Askin, R.A., Hannah, M.J., Mohr, B.A.R., Raine, J.I., Harwood, D.M., Florindo, F., and the SMS Science Team, 2009, Palynomorphs from a sediment core reveal a sudden remarkably warm Antarctica during the middle Miocene: Geology, v. 37, no. 10, p. 955–958, doi: 10.1130/G30139A.1.
Webb, P.-N., and Wrenn, J.H., 1982, Upper Cenozoic micropaleontology and biostratigraphy of eastern Taylor Valley, Antarctica, *in* Craddock, C., ed., Proceedings of the Third Symposium on Antarctic Geology and Geophysics: Madison, Wisconsin, The University of Wisconsin Press, p. 1117–1122.
Whitehead, J.M., Ehrmann, W., Harwood, D.M., Hillenbrand, C.-D., Quilty, P.Q., Hart, C., Taviani, M., Thorn, V., and McMinn, A., 2006, Late Miocene paleoenvironment of the Lambert graben embayment, East Antarctica, evident from: Mollusc paleontology, sedimentology and geochemistry: Global and Planetary Change, v. 50, no. 3–4, p. 127–147.
Wilson, G., Pekar, S., Naish, T., Passchier, S., and DeConto, R., 2009, The Oligocene-Miocene boundary—Antarctic climate response to orbital forcing, *in* Florindo, F., and Seigert, M., eds., Antarctic Climate Evolution: Developments in Earth & Environmental Sciences, Volume 8: Amsterdam, The Netherlands, Elsevier, p. 444–465.
Zachos, J., Pagani, M., Sloan, L., Thomas, E., and Billups, K., 2001, Trends, rhythms, and aberrations in global climate: 65 Ma to present: Science, v. 292, p. 686–693.
Zachos, J.C., Dickens, G.R., and Zeebe, R.E., 2008, An early Cenozoic perspective on greenhouse warming and carbon-cycle dynamics: Nature, v. 451, p. 279–283, doi: 10.1038/nature06588.

Science Editor: Nancy Riggs
Associate Editor: Christine Siddoway

Manuscript Received 17 May 2010
Revised Manuscript Received 13 October 2010
Manuscript Accepted 16 November 2010

Printed in the USA